
Article:
Binti Mohd Najib, N, Somjit, N orcid.org/0000-0003-1981-2618 and Hunter, I orcid.org/0000-0002-4246-6971 (2018) Design and Characterisation of Dual-Mode Suspended-Substrate Stripline Filter. IET Microwaves, Antennas and Propagation, 12 (9). pp. 1526-1531. ISSN 1751-8725

https://doi.org/10.1049/iet-map.2017.1136

Design and Characterisation of Dual-Mode Suspended-Substrate Stripline Filter

Journal:	*IET Microwaves, Antennas & Propagation*
Manuscript ID	MAP-2017-1136.R1
Manuscript Type:	Research Paper
Date Submitted by the Author:	20-Feb-2018
Complete List of Authors:	Binti Mohd Najib, Norazwana; UNIVERSITY OF LEEDS, ELECTRONIC AND ELECTRICAL ENGINEERING Somjit, Nutapong; University of Leeds, School of Electronic and Electrical Engineering Hunter, Ian; University of Leeds, Electronics and Electrical Engineering
Keyword:	MICROWAVE FILTERS, STRIP LINE FILTERS, BAND-PASS FILTERS, PASSIVE FILTERS

Design and Characterisation of Dual-Mode Suspended-Substrate Stripline Filter

Norazwana*, Nutapong Somjit, Ian Hunter

Pollard Institute, Electrical and Electronic Engineering Department, University of Leeds, Leeds LS2 9JT, West Yorkshire, United Kingdom
*elnmn@leeds.ac.uk

Abstract: A new design technique of a dual-mode ring-resonator suspended-substrate stripline filter is reported in this paper to achieve low passband insertion loss, high quality factor and good spurious response. A fourth-order bandpass filter was designed and fabricated at the operational frequency of 2.07 GHz with two ring resonators packaged in a metallic cavity where each ring resonator is one wavelength long. The transmission zeros of the dual-mode filter are generated due to the phase cancellation between the two paths in a ring, thus a sharp-skirt selectivity filter response was achieved. Perturbation notch structure was implemented on each ring resonator to provide the electromagnetic coupling of two degenerate modes, thus a dual-mode response of the filter can be synthesized. Measurement results of the first dual-mode filter prototype showed a return loss and an insertion loss of better than 16.42 dB and 0.926 dB, respectively, while an out-of-band rejection of up to 55 dB was achieved. The novel filter design technique proved that no cross-coupling is required to obtain the transmission zeros of the filter, thus the sharp-skirt response was achievable.

1. Introduction

In cellular-radio base stations, signals are being transmitted and received simultaneously. In the receive band, there are chances of intermodulation products from the power amplifier being fed to the receiver, thus the transmit filter must have a very high level of signal rejection [1]. Furthermore, the transmit filter must also have low passband insertion loss because it impacts the power transmitted and the overall transmit system efficiency. Recently, filters with a dual-mode operation have been investigated due to their ability to produce two degenerate modes using a single physical structure; therefore, the size and cost of the filter can be reduced without compromising any figures-of-merit.

There are many research studies improving the design of the transmit filter by using the dual-mode design technique. The microstrip technology is frequently used in designing dual-mode filters due to its advantages, such as low profile and fabrication cost. A dual-mode rotational symmetric resonator filter was developed with two transmission zeros generated near the upper and lower passband [2]. In addition, a fourth-order dual-mode microstrip filter with interdigital capacitive loading element was developed [3]. In [4] and [5], compact dual-mode microstrip filters were designed, fabricated and evaluated by using a parallel coupled resonator and meander loop resonator, respectively. Furthermore, a triangular microstrip dual-mode filter based on the coupling matrix synthesis method was developed with a good rejection performance obtained [6]. In addition, a dual-mode filter with source-load coupling was designed in [7] and [8] demonstrated good filter performance. All previously mentioned microstrip dual-mode filter designs offer good return loss and sharp-skirt selectivity due to their ability to generate transmission zeros. Nonetheless, they suffered high insertion loss, which is on average approximately higher than 1 to 2 dB at midband frequency.

The suspended-substrate stripline technology offers various attractive advantages, which are comparable to a microstrip or other planar transmission lines. Filtering circuits implemented using suspended-stripline structures achieve high signal selectivity, lower insertion loss and good temperature stability. This is because the suspended-stripline technology uses the air as the dielectric material to connect to the ground plane, thus minimising the signal transmission losses associated with dielectric material loss. Another key advantage of the suspended-stripline structure is that the circuit patterns can be printed on both sides of the stripline substrate, which enables strong broadside electromagnetic (EM) coupling, as well as the use of a metal housing that prevents the EM fields of the filter from radiating loss. Because suspended stripline is a purely transverse electromagnetic (TEM) transmission-line structure, it is non-dispersive, and thus makes the suspended stripline an interesting structure for high-performance filters. Presently, only a dual-mode suspended-substrate stripline was demonstrated using quarter-wave resonator and inductor [9]. However, it was designed for broadband frequency and the insertion loss and return loss obtained were worse than 1 dB and 10 dB in the passband frequencies, respectively.

This paper reports on developing a new design of dual-mode suspended-substrate stripline filter to achieve low passband insertion loss, high quality factor (Q) and good spurious response without compromising any other figures-of-merit. The filter is designed to operate at 2.07 GHz with a bandwidth of 50 MHz while the requirements of the return loss of better than 15 dB and insertion loss of less than 1 dB

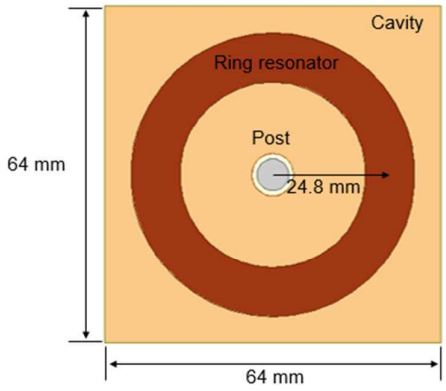

Fig. 1 *Top view of a ring resonator structure with a metal post shorted to ground.*

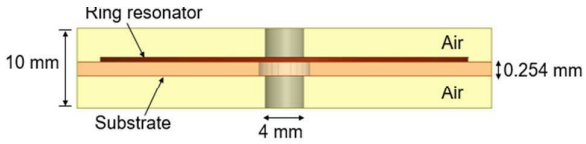

Fig. 2 *Front view of a ring resonator structure with a metal post shorted to ground.*

are desired. A fourth-order bandpass filter was designed with two ring resonators packaged in a metallic cavity housing, where each ring resonator was designed to be one wavelength long. Because of the phase cancellation between two paths in a ring, the transmission zeros can be fully controlled and generated, thus a sharp-skirt selectivity filter response is achieved. In this new design technique, no cross-coupling is needed to achieve a high-selectivity filter response. Moreover, a perturbation notch is implemented on the ring resonators to provide the coupling of two degenerate modes, thus dual-mode responses can be synthesized. Therefore, this new design technique solves the disadvantage of the conventional suspended-substrate stripline technology. The designed dual-mode suspended-substrate filter was fabricated and measured. A return loss of better than 16 dB, an insertion loss of < 1 dB and a bandwidth of 58 MHz was achieved, which agree well with the simulation outcome.

2. Dual-Mode Ring-Resonator Filter

Table 1 Simulated Eigenmode solution for ring without metal post

Eigenmode	Frequency (GHz)	Unloaded Q
Mode 1	2.07	1486.26
Mode 2	2.07	1496.46
Mode 3	3.34	4654.81

To investigate the harmonic suppression effect, a wavelength-long dual-mode ring-resonator filter was designed and simulated at 2.07 GHz. Fig. 1 and Fig. 2 depict the top and front views of the ring-resonator filter with a metal post

Table 2 Simulated Eigenmode solution for ring with metal post

Eigenmode	Frequency (GHz)	Unloaded *Q*
Mode 1	2.07	1569.43
Mode 2	2.07	1528.28
Mode 3	4.06	2211.79

Table 3 Simulated Eigenmode solution for various post radius

Post radius (mm)	Mode 1 Frequency (GHz)	Mode 3 Frequency (GHz)	Unloaded *Q*
1	2.07	4.02	1596.13
2	2.07	4.06	1569.43
3	2.07	4.05	1557.60
4	2.07	4.05	1524.55
5	2.07	4.06	1566.53

implemented at the centre of the ring resonator, respectively. The metal post is placed at the centre of the cavity to create a short circuit to the ground plane and used to improve the first harmonic of the ring-resonator filter. Rogers RT/Duroid

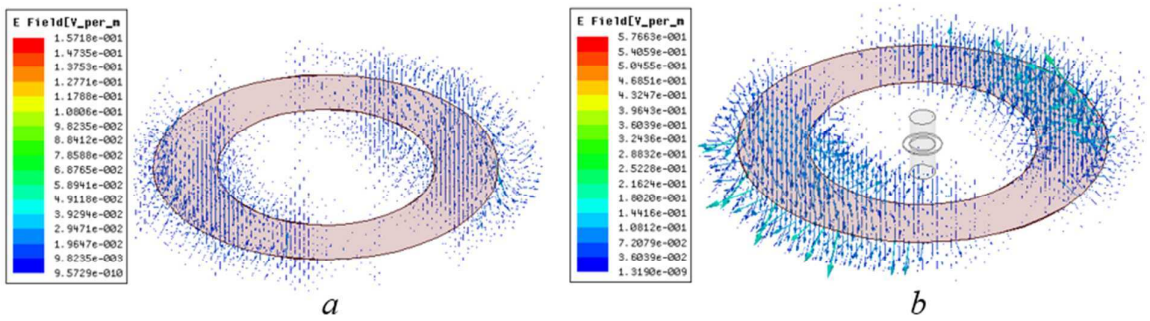

Fig. 3 *Electric field distribution for mode 1 of a ring resonator (a) without and (b) with a metal.*

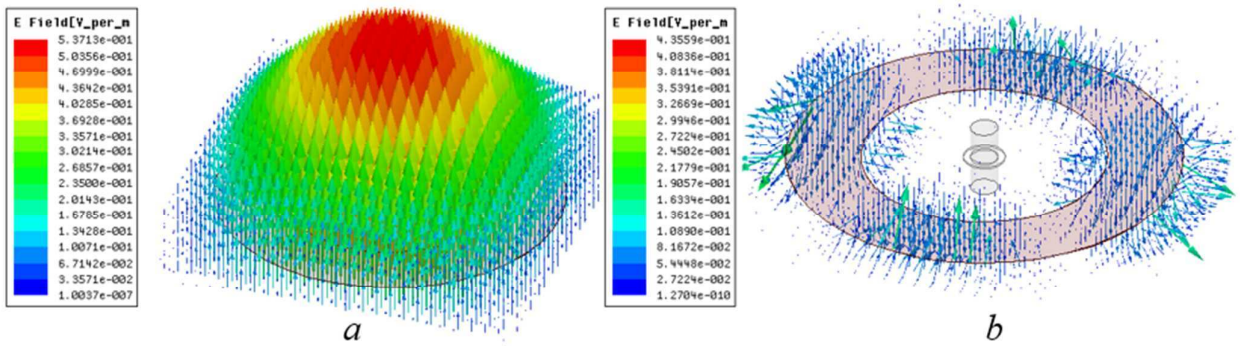

Fig. 4 *Electric field distribution for mode 3 of a ring resonator (a) without and (b) with a metal.*

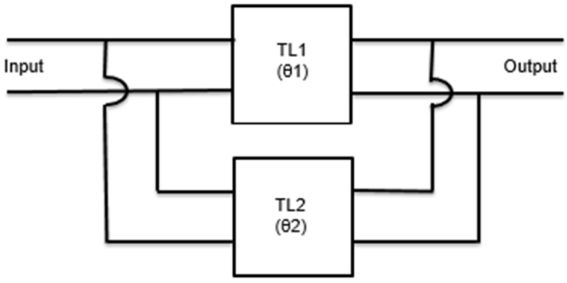

Fig. 5 *Equivalent circuit representation of the ring resonators.*

5880 with dielectric constant ε_r = 2.2 and thickness h = 0.254 mm was selected as the substrate for the filter design. A full-wave EM simulator (HFSS) was used to investigate and synthesize the dual-mode resonance frequency and harmonics [10]. Tables 1 and 2 represents the simulated eigenmode solution of a ring-resonator design without and with a metal post shorted to ground. The first harmonic frequency and Q-factor are improved from 3.34 GHz to 4.05 GHz and from 1486.26 to 1569.43, respectively, when the metal post is implemented in the dual-mode filter design. This is because the electric-field distribution at the centre of the cavity was pushed towards the ring edges due to the metal post, thus increasing the frequency distance of the first harmonic frequency. Table 3 presents the simulated eigenmode solution for the post radius, which is varied from 1 mm to 5 mm. Three parameters are observed in the simulation, namely the mode 1 frequency, mode 3 frequency and the unloaded quality factor. From the simulation outcome, it was observed that no significant change was seen in all the three parameters when the post radius is changed up to 5 mm. The small changes will not have much effect on the simulated frequency response of the designed filter. Therefore, a 2 mm radius post was chosen to be used in the designed filter. Fig. 3 shows the electric-field distribution of EM mode 1 of the ring resonator without and with a metal post at the centre of the resonator structure. Fig. 4 shows the electric-field distribution of mode 3 of the ring resonator without and with a metal post at the centre of the resonator structure. For this case, the electric-field distribution of this mode was pushed away from the centre of the cavity when a metal post was implemented at the centre of the ring-resonator structure. Therefore, the simulation results show that a wider out-of-band rejection, is achievable by adding the metal post at the centre of the ring-resonator structure. Therefore, a filter design technique based on ring-resonator structure with a metal post at the centre of the resonator is utilised for a superior dual-mode filter design.

Fig. 6 *Equivalent circuit representation for the two-port network.*

3. Analysis and Design of the Dual-Mode Filter

The ring resonator was analysed as two transmission lines with electrical length of $\theta_1$and θ_2 connected in parallel as shown in Fig. 5, where the characteristic impedances Z_0 of the transmission lines are assumed to be 1 Ω. The *Y*-matrix of the transmission line is:

$$[Y] = \begin{bmatrix} \frac{-j}{\tan\theta} & \frac{j}{\sin\theta} \\ \frac{j}{\sin\theta} & \frac{-j}{\tan\theta} \end{bmatrix} \quad (1)$$

Because the two transmission lines are connected in parallel, therefore, we get:

$$[Y] = j\begin{bmatrix} -\frac{1}{\tan\theta_1} - \frac{1}{\tan\theta_2} & \frac{1}{\sin\theta_1} + \frac{1}{\sin\theta_2} \\ \frac{1}{\sin\theta_1} + \frac{1}{\sin\theta_2} & -\frac{1}{\tan\theta_1} - \frac{1}{\tan\theta_2} \end{bmatrix} \quad (2)$$

If the *Y*-matrix is presented as a π network, the equivalent circuit of the two-port network is pictured in Fig. 6 where the π network is represented as admittance inverter K_{12}. Therefore

$$jK_{12} = y_{12} \quad (3)$$

And from (2)

$$y_{12} = \frac{j}{\sin\theta_1} + \frac{j}{\sin\theta_2} \quad (4)$$

Hence, the transmission zeros of this matrix are the zeros of y_{12} and occur when

$$\sin\theta_1 + \sin\theta_2 = 0 \quad (5)$$

The external coupling is also referred to as input and output coupling. The external quality factor (Q_e) was first calculated from

$$Qe = \frac{f_o}{BW\ x\ {M_{S1}}^2}, \quad (6)$$

where f_o, BW and M_{S1} are the operating frequency, bandwidth and normalized coupling value, respectively. The normalized coupling value is extracted from the coupling matrix synthesis software (CMS) [11] based on the desired specification requirements. The input and output coupling depends on the gap distance between the input/output feeding transmission line and the ring resonator. The exact gap distance for the input and output coupling are determined from the external quality factor (Q_e) versus gap distance graph as shown in Fig. 7.

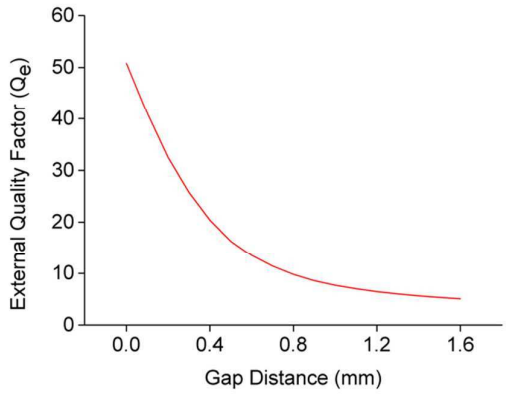

Fig. 7 *External quality factor (Q_e) versus gap distance.*

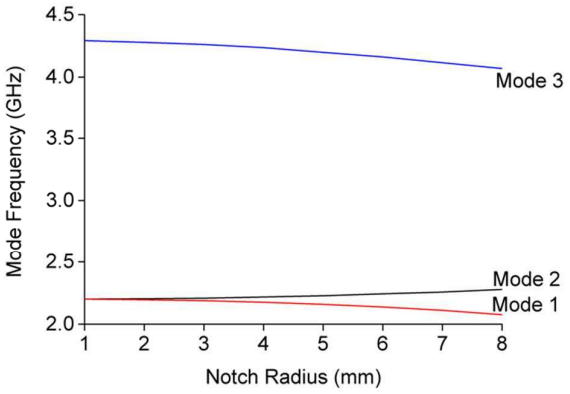

Fig. 8 *Mode splitting frequency for various notch radii.*

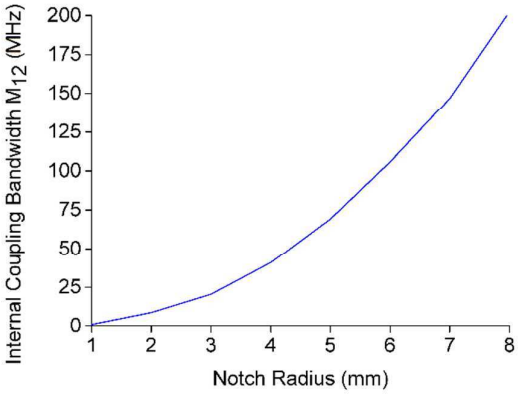

Fig. 9 *Internal coupling bandwidth versus notch radius.*

The normalized coupling constants of mode 1–2 and mode 3–4 which are referred to as M_{12} and M_{34}, respectively, are defined and controlled by the perturbation size of the ring resonators. The new dual-mode filter design is initially under weak capacitive coupling with a perturbation located 135° to the input and output feeding port of the ring resonators to investigate the influence of varying the notch radius to the dual-mode filter response. The location and size of the notch of the ring resonators are two important design parameters, where it influences the electrical filter performance. Fig. 8 depicts the relations between the first three resonant modes and notch radius of the ring resonators. As the notch radius increases, one of the degenerate modes remains unchanged while the other one slowly moves downwards, thus separating these two modes from each other. Therefore, the notch radius controls the mode splitting of the degenerate modes. Fig. 9 represents the plot of the relationship between the coupling bandwidth and the notch radius. The wider filter bandwidth is achievable with the increasing notch radius of the ring resonators. Hence, a suitable notch radius can be chosen to split the two degenerate modes based on the required coupling bandwidth obtained from [11].

The coupling constant between two rings is referred to as M_{23}, which is controlled by the gap spacing between the metal strip and the two rings. The inter-ring coupling value was first extracted from [9]. The ring resonators were initially loosely coupled and the inter-ring coupling was adjusted until S_{21} between two peaks is roughly –30 dB to –40 dB to synthesize loose coupling. The inter-ring coupling was computed from [12] with

$$K = \frac{{f_H}^2 - {f_L}^2}{{f_H}^2 + {f_L}^2}, \quad (7)$$

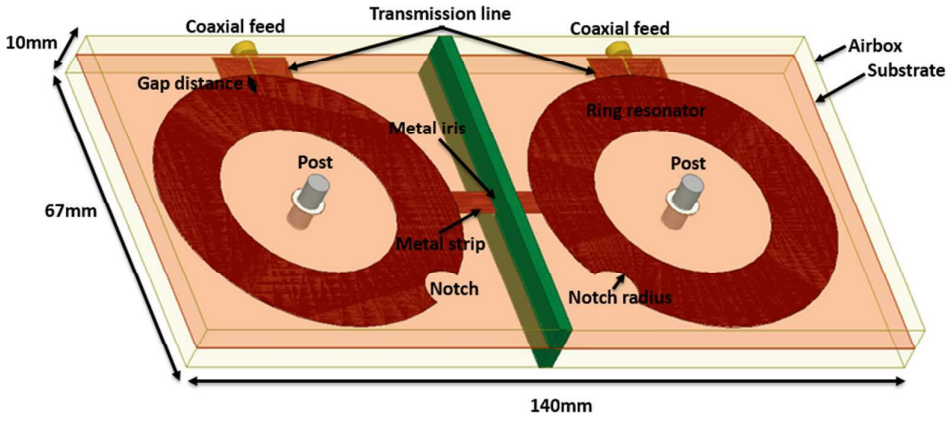

Fig. 10 *Fourth-order filter layout.*

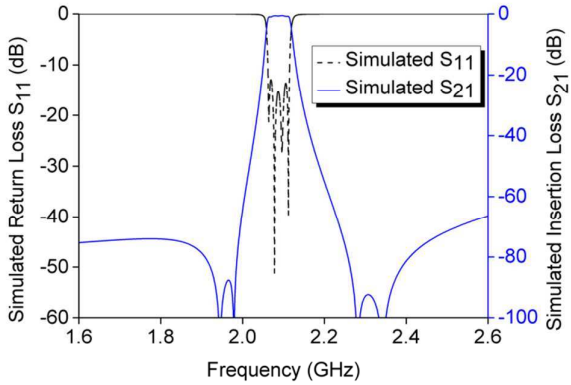

Fig. 11 *Simulated frequency response of the fourth-order filter.*

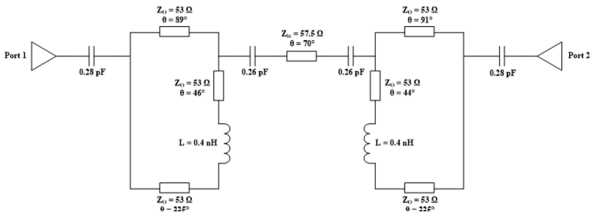

Fig. 12 *Transmission line equivalent circuit of the fourth-order filter.*

where f_H is frequency of the upper peak while f_L is the frequency of the lower peak.

4. Fourth-Order Filter Design

A fourth-order bandpass filter is designed at the operational frequency of 2.07 GHz and a bandwidth of 50 MHz as depicted in Fig. 10. The green box is the metal iris from the housing, which is used to avoid unwanted cross-coupling between the two rings. The overall dual-mode filter length, width and height are 140 mm, 67 mm and 10 mm, respectively. Fig. 11 shows the simulation result of the dual-mode filter with a return loss of better than 15.33 dB and an insertion loss of approximately 0.66 dB at the centre

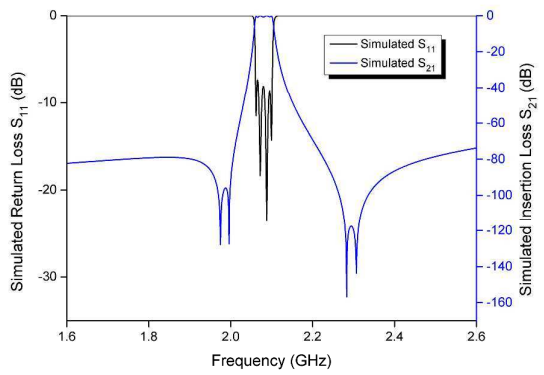

Fig. 13 *Simulated frequency response of the transmission line equivalent circuit*

frequency of 2.088 GHz. Besides, the two pairs of transmission zeros are synthesized to be below and above the passband with a band rejection of up to 74 dB because when a ring was fed at 90°, two separate paths exist with one path of $\lambda/4$ while the other one is $3\lambda/4$ in which it creates 180°-phase difference. The 180°-phase difference thus naturally creates zero transmissions of the dual-mode filter design. Although the size of the two rings is identical, the transmission zeros appeared at four different frequencies. This is because there is more than one solution available for the transmission zero, which referred to equation (5). This is proven by the transmission-line equivalent circuit of the fourth-order filter as shown in Fig. 12. The difference in the electrical length of both rings has led to the formation of four transmission zeros, even though the values of the characteristic impedances of both rings are the same. The simulated frequency response of the transmission-line equivalent circuit is shown in Fig. 13 where four transmission zeros were observed. Fig.14 shows the measurement result of the fabricated filter with a return loss of approximately 16.42 dB, an insertion loss of better than 0.926 dB and a bandwidth of 57.7 MHz. Two pairs of transmission zeros were observed in the measurement results, which agreed well with the simulation outcomes. A

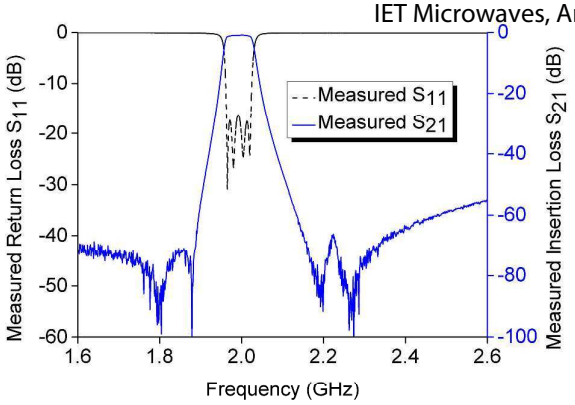

Fig. 14 *Measured frequency response of the fabricated fourth order filter*

shifting in the resonance frequency is caused by the tuning screws and fabrication tolerance.

Fig. 15 shows a wideband frequency response of the fabricated filter where approximately 1.2 GHz spurious free band is observed. The first harmonic appeared at 3.53 GHz, which is nearly double the fundamental frequency. Fig. 16 and Fig. 17 represent the top and bottom layer of the

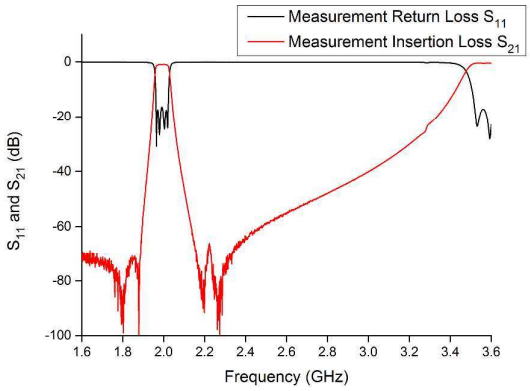

Fig. 15 *Wideband frequency response of the fabricated fourth-order filter.*

fabricated filter, respectively, where the ring resonators are fabricated on the top layer while the coupling strip and transmission lines are implemented on the bottom layer.

5. Conclusion

In this paper, a fourth-order dual-mode suspended-substrate stripline filter has been presented where the influence of metal post was investigated. The first harmonic was suppressed at nearly double the fundamental frequency by adding a metal post. Using 90° input and output port arrangement with notches, the dual-mode response was generated. Moreover, the transmission zeros were generated due to the phase difference between two paths in a ring, thus a sharp-skirt selectivity response was achieved. The obtained frequency response indicated that the dual-mode suspended-substrate stripline filter enables the achievement of low-loss filter response, good spurious, high *Q*-factor as well as high selectivity without any cross-coupling connection.

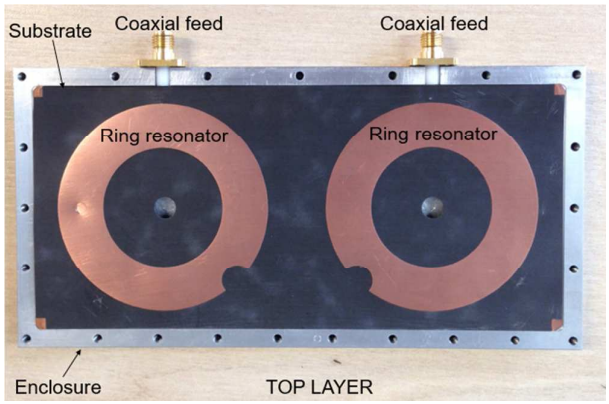

Fig. 16 *Top layer of the fabricated fourth-order filter.*

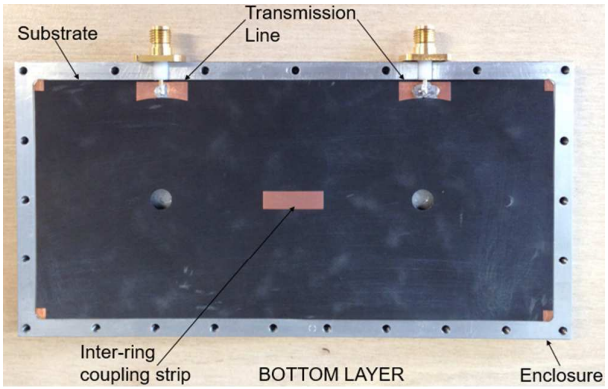

Fig. 17 *Bottom layer of the fabricated fourth order filter.*

6. References

[1] R. R. Mansour, 'Filter technologies for wireless base stations,' *IEEE Microw. Mag.*, vol. 5, pp. 68–74, 2004.

[2] S. S. Gao, H. L. Liu, J. Li, and W. Wu, 'A compact dual-mode bandpass filter for GPS, Compass (Beidou) and GLONASS,' *10th Glob. Symp. Millimeter-Waves, GSMM 2017*, pp. 28–30, 2017.

[3] C. Karpuz, P. Ö. Özdemir, and G. B. Fırat, 'Design of Fourth Order Dual-Mode Microstrip Filter by Using Interdigital Capacitive Loading Element with High Selectivity,' pp. 461–464, 2016.

[4] C. J. Chen, 'Design of Parallel-Coupled Dual-Mode Resonator Bandpass Filters,' *IEEE Trans. Components, Packag. Manuf. Technol.*, vol. 6, pp. 1542–1548, 2016.

[5] T. Y. Y. Xiang, T. Lei, M. Peng, T. Lei, and M. Peng, 'Miniature dual-mode bandpass filter based on meander loop resonator with source-load coupling,' in *2015 Asia-Pacific Microwave Conference (APMC)*, 2015, vol. 3, pp. 1–3.

[6] L. Zhang, Z. Qi, J. Chu, and X. Li, 'Design of triangular microstrip dual mode filter based on the coupling matrix synthesis method,' *9th Int. Conf. Microw. Millim. Wave Technol. ICMMT 2016 - Proc.*, vol. 1, no. 1, pp. 235–237, 2016.

[7] J. Wang, J. Li, J. Ni, S. Zhao, W. Wu, and D. Fang, 'Design of Miniaturized Microstrip Dual-Mode Filter With Source-Load Coupling,' vol. 20, no. 6, pp. 319–321, 2010.

[8] L. Li and Z.-F. Li, 'Application of inductive source-load coupling in microstrip dual-mode filter design,' *Electron. Lett.*, vol. 46, no. 2, p. 141, 2010.

[9] J. S. Kim, N. S. Kim, W. G. Moon, and L. Gyu-Bok, 'Novel broadband suspended substrate stripline filter using dual-mode resonators,' in *2008 IEEE 19th International Symposium on Personal, Indoor and Mobile Radio Communications*, 2008, pp. 1–4.

[10] ANSOFT, *An Introduction to HFSS: Fundamental Principles, Concepts, and Use*. 2009.

[11] G. W. Technology, *CMS-Filter & Coupling Matrix Synthesis Software*. 2013.

[12] H. Jia-Sheng and M. J. Lancaster, *Microstrip Filters for RF/Microwave Applications*. United States of America: John Wiley & Sons, Inc., 2001.